Journal of Rehabilitation in Civil Engineering 6-1 (2018) 88-103

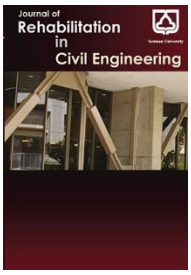

journal homepage: http://civiljournal.semnan.ac.ir/

An Artificial Neural Network Model for Estimating the Shear Contribution of RC Beams Strengthened by Externally Bonded FRP

E. Moradi[1], H. Naderpour[2*] and A. Kheyroddin[3]
1. M.Sc. Student, Faculty of Civil Engineering, Semnan University, Semnan, Iran
2. Associate Professor, Faculty of Civil Engineering, Semnan University, Semnan, Iran
3. Professor, Faculty of Civil Engineering, Semnan University, Semnan, Iran

Corresponding author: *naderpour@semnan.ac.ir*

ARTICLE INFO

Article history:
Received: 28 January 2014
Accepted: 08 June 2014

Keywords:
RC Beams,
Shear,
FRP Bond,
ANN.

ABSTRACT

This paper provides an artificial neural network model for predicting the shear contribution of FRP in reinforced concrete (RC) beams strengthened in shear with externally bonded FRP. Although there are some models and equations for estimating the contribution of FRP, these models, in some cases, have a significant error in the calculation of FRP contribution. One of the reasons for these errors is neglecting the effect of shear span (a) to the effective depth of beam (d) ratio in FRP performance. In this model, mechanical and dimensional properties of RC beams strengthened and strengthening materials, and also the shear span to the effective depth of beam ratio (a/d) are taken as input parameters, and the shear contribution of FRP is the target of the network. After a comprehensive review in existing literature, 96 strengthened RC beams which all of them have FRP rupture failure mode were selected which 92 of them were used for training, validation and testing the network and four of them were used for controlling the generalization of the network. Finally, the outputs of the model have compared with ACI 440.2R, fib 14 and CIDAR guidelines, and the result indicated that the ANN model is more accurate than the existing guideline equations based on experimental result.

1. Introduction

Nowadays, deterioration condition of the existing reinforced concrete (RC) structures, is one of the main anxiety of the modern communities. in the last decade, strengthening of RC structure usually uses to do by epoxy bonding of steel plates on the face of concrete elements, increasing the element section by placing extra reinforced

DOI: 10.22075/JRCE.2018.376.1072

and casting concrete around the existing section [1,2]. In recent years, considerable research has been conducted on the use of fiber-reinforced polymer (FRP) for strengthening exciting structures. FRP materials due to best performance and enhancement of strength and ductility have been highly regarded, and many experimental studies have been carried out on the use of these materials [3-12].

Although the shear failure of RC beams is sudden, brittle, and without any warning in nature [3], most of the studies on strengthening have conducted on flexural strengthening. Using epoxy-bonding of FRP composites on side faces of RC beams, brittle behavior changes to ductile behavior [4].

The first study in shear strengthening of RC beams with FRP was performed by Berset [5]. He tested some RC beams in both of control specimens and FRP-strengthened specimens type and developed a simple analytical model for shear contribution of FRP composite, which in this model, FRP treated similar to steel stirrups. Uji [6] tested RC beams strengthened by FRP with bonding FRP on their side faces either vertical or inclined. In this study, Uji focused on debonding shear stress. In another work, Veilhaber and Limberger [7] tested some large scale RC beams, and the test results indicated that even small amounts of external reinforcement could avoid brittle shear failure. Chajes *et al.* [8] tested 12 beams, four as control specimens and eight as strengthened RC beams with aramid, E-glass, and graphite fibers. The tests results indicated that FRP composite increases in the ultimate strength of about 60 to 150 percent. Sato *et al.* [9] tested some RC beams with shear strengthening by FRP strips or continuous fabrics, and the result of tests indicated that the effect of partial strengthening on the shear contribution of composite materials. Gamino [10] has tested some RC beams for investigating the effect of anchorage for avoiding FRP-debonding. The results of another study have been showed that the strain values in FRP increase only after the appearance of the shear crack crossing the FRP wraps [11]. Jung-Yoon Lee *et al.* [12] tested ten RC beam strengthened with FRP for investigating the effective strain of composite material, and the test results indicated that the effective strain of FRP at shear failure decreased as the amount of FRP increased or as the apace of FRP strips decreased.

In recent years, artificial neural networks have been of interest to researchers in the utilizing of various civil engineering fields [13]. ANN tools are an efficient method for further understanding of the behavior of RC members and concrete. Since the shear failure of RC beams involves a complex mechanism and the capacity of FRP in shear strengthened RC beams depends on different parameters, usage of Artificial Neural Network (ANN) can help to predict the ultimate contribution of FRP composite.

2. Existing Models of RC Beam Shear Strengthening

Although numerous studies have been conducted on the shear capacity of the strengthened RC beams, because of complicated mechanism of shear failure, the precision of existing models is not appropriate to predict the shear contribution of FRP materials.

The following shear models commonly applied in practical design and researches. These models have used for comparing the result of proposed model based on experimental database [Table 1-4]. Presented equations in ref. 14-17 are the most common standard for calculating the shear contribution of FRP materials, and their formulas have been used for comparison with the experimental result against the result of the ANN model presented in this paper.

3. Artificial Neural Networks

Artificial neural networks (ANN) are computing tools for modeling complex problems inspired by biological neurons. A biological neuron has major parts which are of particular interest in understanding an artificial neuron and include: dendrites, soma, axon, and synapse. The first wave of interest in neural networks emerged after the introduction of simplified neurons by McCulloch and Pitts in 1943s. The analogy between biological and artificial neural networks was shown in Table 5. These neurons are connected with a connection link in each layer.

The training operation of a network is done by adjusting the values of the weights between layers. At each epoch, the network output is computed based on weigh coefficients and was compared with the real value. According to the error rate, the network weight is adjusted until the network output matches the target value. The feedforward backpropagation network is one of the simple various ANN that has the appropriate ability to modeling complex function. Backpropagation is the generalization of the Widrow–Hoff learning rule to multiple-layer networks and nonlinear differentiable transfer functions. Feedforward networks often have one or more hidden layers of sigmoid transfer functions associated with a linear in the output layer.

Nowadays, the results of the parametric study that carried out on the various field of structural engineering using artificial neural networks were shown the capability of this tolls [13, 20, 21].

Table 1. ACI 440 [14] shear calculation equations.

$$V_f = \frac{A_{fv} f_{fe} d_{fv} (sin\alpha + cos\alpha)}{s_f} \quad , \quad A_{fv} = 2nt_f w_f \quad , \quad f_{fe} = \varepsilon_{fe} E_f$$

$$\varepsilon_{fe} = 0.004 \le 0.75\varepsilon_{fu} \qquad \textit{for fully wrapped}$$

$$\varepsilon_{fe} = K_v \varepsilon_{fu} \quad , \; K_v = \frac{k_a k_2 L_e}{11{,}900\,\varepsilon_{fu}} \; , \qquad \textit{for } U-\textit{jacketing}$$

$$L_e = \frac{23{,}300}{(nt_f E_f)^{0.58}} \quad , \quad k_1 = \left[\frac{f_c'}{27}\right]^{2/3} \quad , \quad k_2 = \frac{d_f - L_e}{d_f}$$

Table 2. *fib* 14 [15] shear calculation equations.

$$V_{fd} = 0.9\varepsilon_{fd,e} E_{fu} \rho_f b_w d\left(cot\ \theta + cot\ \alpha\right) sin\ \alpha$$

$$\rho_f = 2\frac{t_f}{b_f} sin\alpha \quad continuous\ strengthening, \quad \rho_f = 2\frac{t_f}{b_f}\frac{w_f}{s_f} \quad strengthening\ with\ strips$$

$$\varepsilon_{fe} = 0.17\left[\frac{f_{cm}^{2/3}}{E_{fu}\rho_f}\right]^{0.30} \varepsilon_{fu} \qquad for CFRP\ without\ debonding$$

$$\varepsilon_{fe} = 0.048\left[\frac{f_{cm}^{2/3}}{E_{fu}\rho_f}\right]^{0.47} \varepsilon_{fu} \qquad for\ AFRP\ without\ debonding$$

Table 3. CIDAR [16] shear calculation equations.

$$V_f = 2 f_{fed}.t_f.\frac{w_f}{s_f}.h_{fe}.(\cot\theta + \cot\alpha)\sin\alpha\ ; \quad h_{fe} = z_b - z_t\ ; \quad z_b = 0.9d - d_{fb}\ ; \quad z_t = d_{ft}\ ; \quad f_{fed} = D_f \cdot f_{fd,\max}$$

$$fully\ wrapped \left\{ f_{fd,\max} = \begin{cases} \frac{1}{\gamma_f}.\phi_R.f_{fu}; & \varepsilon_f \le 1.5\% \\ \frac{1}{\gamma_f}.\phi_R.E_f.\varepsilon_f; & \varepsilon_f > 1.5\% \end{cases} , \quad D_f = 0.5\left(1+\frac{z_t}{z_b}\right) \right\}$$

$$U-shape\ strengthening \left\{ \begin{array}{l} f_{fd,\max} = \min\left\{ \begin{array}{l} \frac{1}{\gamma_f}.\phi_R.f_{fu} \\ \frac{1}{\gamma_f}\cdot 0.35\cdot\beta_L\cdot\beta_w\cdot\sqrt{\frac{E_f\cdot\sqrt{f_{ck}}}{f_t}} \end{array} \right. , \quad D_f = \begin{cases} \frac{2}{\pi\cdot\lambda}\cdot\frac{1-\cos\left(\frac{\pi}{2}\cdot\lambda\right)}{\sin\left(\frac{\pi}{2}\cdot\lambda\right)}; & \lambda \le 1 \\ 1-\frac{\pi-2}{\pi\cdot\lambda}; & \lambda > 1 \end{cases} \\ \beta_L = \begin{cases} \lambda, & \lambda \le 1 \\ 1, & \lambda > 1 \end{cases} , \quad \beta_w = \sqrt{\frac{2-w_f/(s_f\cdot\sin\alpha)}{1+w_f/(s_f\cdot\sin\alpha)}} , \quad \lambda = \frac{L_{\max}}{L_e} , \quad L_{\max} = \frac{h_{fe}}{\sin\alpha} , \quad L_e = \sqrt{\frac{E_f\cdot t_f}{\sqrt{f_{ck}}}} \end{array} \right.$$

Table 4. JSCE [17] shear calculation equations.

$$V_{fd} = K.[A_f.f_{fud}(\sin\alpha_f + \cos\alpha_f)/s_f].(z/\gamma_b)$$

$$K = 1.68 - 0.67R \quad , \quad 0.4 \le K \le 0.8$$

$$R = (\rho_f.E_f)^{1/4}\left(\frac{f_{fud}}{E_f}\right)^{2/3}\left(\frac{1}{f'cd}\right)^{1/3} , \quad 0.5 \le R \le 2.0$$

$$\rho_f = A_f/(b_w.s_f) = (t_f.w_f)/(b_w/s_f) = \left(\frac{w_f}{s_f}\right)\left(\frac{t_f}{b_w}\right)$$

Table 5. The analogy between biological and artificial neural networks.

Biological Neural Network	Artificial Neural Network
Soma	Neuron
Dendrite	Input
Axon	Output
Synapse	Weight

4. Neural Network Model

As the first step for providing a sufficient group of data for training, verifying and testing of the neural network, a comprehensive review has done among existing papers in shear strengthening of RC beams and a set of the test result on shear strengthening of RC beams by FRP composites was collected. Although at first the data set involved more than 300 strengthened RC beams, they had a different type of failure; like FRP rupture, debonding, and flexural failure. So for training a reasonable network that can predict the shear contribution of FRP at ultimate load, altogether about one-third of tests (96 specimens) which have FRP rupture failure were chosen. 92 specimens of whole data were selected for training, validation, and testing the network and four specimens for controlling the result of the network.

For using the ANN method for estimating the shear contribution of FRP in shear strengthened RC beams, choosing the appropriate parameters is a significant remarkable factor. At first, ten parameters were determined based on physical considerations as input parameters of the network. For choosing these parameters, existing models and equations in shear strengthening of RC beams have been studied, and the following parameters have been selected:

ultimate FRP strain (ε_{fu}), effective depth of FRP (d_f), width of FRP strips (w_f), center to center spacing of FRP strips (s_f), the angle between fiber direction and beam axis (α), concrete compressive strength (f'_c), effective depth of RC beam (d), modulus of elasticity of FRP (E_f) and FRP thickness (t_f) are the effective parameters in FRP performance. In addition to these nine parameters, shear span (a), is another parameter which can determine the type of beam (slender beam or deep beam) and play a forcible role in FRP contribution [12].

From another point of view, for training a good network, whatever input parameters are fewer, the results will be better [20]. So after a comprehensive and carefully investigation between different models and guidelines, some of the mentioned parameters have been incorporated for decreasing the number of input parameters. This process has done, as described in the following:

With due attention to existing equations and models [14-16], the width of FRP strips (w_f) and spacing of FRP strips (s_f) have direct proportion and inverse proportion with FRP contribution respectively. Also increasing the value of ($sin\alpha + cos\alpha$) can improve FRP performance. So these three parameters were incorporated together and make a single parameter.

The modulus of elasticity of FRP (E_f) and FRP thickness (t_f) show the rigidity of composite. According to existing equations, both of these two parameters have a proportion with FRP contribution. So these parameters were incorporated together and make a single parameter.

According to existing research [effect of…], the type of beam (slender or deep) can influence on FRP performance. Shear span (a) to the effective depth of beam (d) ratio is a parameter which shows beam type. So these two parameters were incorporated for making a difference between a slender beam and deep beam.

Finally, ten parameters were changed into six parameters as network input vectors, which are summarized as follow:

(1)The ultimate strain of FRP composite (ε_{fu})

(2)The effective depth of FRP, (d_f)

(3)Width and spacing factor, B = (w_f / s_f).(sin α)

(4)Concrete compressive strength, (f'_c)

(5)FRP rigidity factor, R = E_f . t_f

(6)Shear apan to the effective depth of beam ratio (a/d)

Having the six input parameters as described above, the shear contribution of FRP material was the target node of the neural network. Because of variable scopes of input parameters and target, before training the selected data, scaling for the whole data were done. For scaling, all the data were drawn to their standard values using Eq. (1),(2) and Table 6, which the mean and the standard digression values of scaled data were 0 and 1 respectively. A feed-forward backpropagation type of network was chosen. The Levenberg-Marquardt algorithm was used as network training function, which randomly divides input vectors and target vectors into three sets, including training, validation, and testing. The relative percentage of these sets can be changed. In this study, 70% of whole data was specified as the training data. Also, 15% of database was used as validation data, and remind15% was chosen as testing data randomly.

$$S^2 = \frac{1}{n}\sum_{i=1}^{n}(x_i - \bar{x})^2 \quad (1)$$

$$z_i = \frac{\left(x_i - \bar{x}\right)}{S} \quad (2)$$

Where for each input parameter and target, S^2 is the variance of data, n is the number of data, x_i is the value of the parameter, $\bar{x}$ is the average of the parameter, z_i is the scaled value and S is the root of the variance (standard deviation).

Table 6. Statistics properties of input and target data.

Input parameters	B	ε_f	R (GPa.mm)	a/d	f'_c (MPa)	d_f (mm)	V_f (kN)
Max.	0.08	0.006	3.212	1.25	9.63	88.9	15.4
Min.	1.41	0.037	130.26	4.08	57.27	510	493
Mean	0.66	0.017	36.03	2.73	31.11	276.05	81.47
Variance	0.108	5.281E-5	757.824	0.375	92.17	9762.5	6086/84
Std. dev.	0.329	0.007	27.529	0.613	9.6	98.805	78.02

One hidden layer was used as transfer functions in this ANN model, which it was tangent-sigmoid. The number of neurons in the hidden layer is changeable, and it usually depends on the number of input data. In this study, some networks were created with different numbers of neurons, called ANN-x, which x shows the number of hidden neurons, to find out the optimum number of hidden neurons. The results of each one are indicated in Fig. 2 and 3. As it's clear, the network with eight hidden neurons has the best performance (Fig. 2, 3). Fig. 4 indicates the architecture of a network with eight neurons in the hidden layer. Although increasing the number of hidden neurons usually makes the network give better results, if the number of hidden neurons be very high, it can cause the problem of over-fitting.

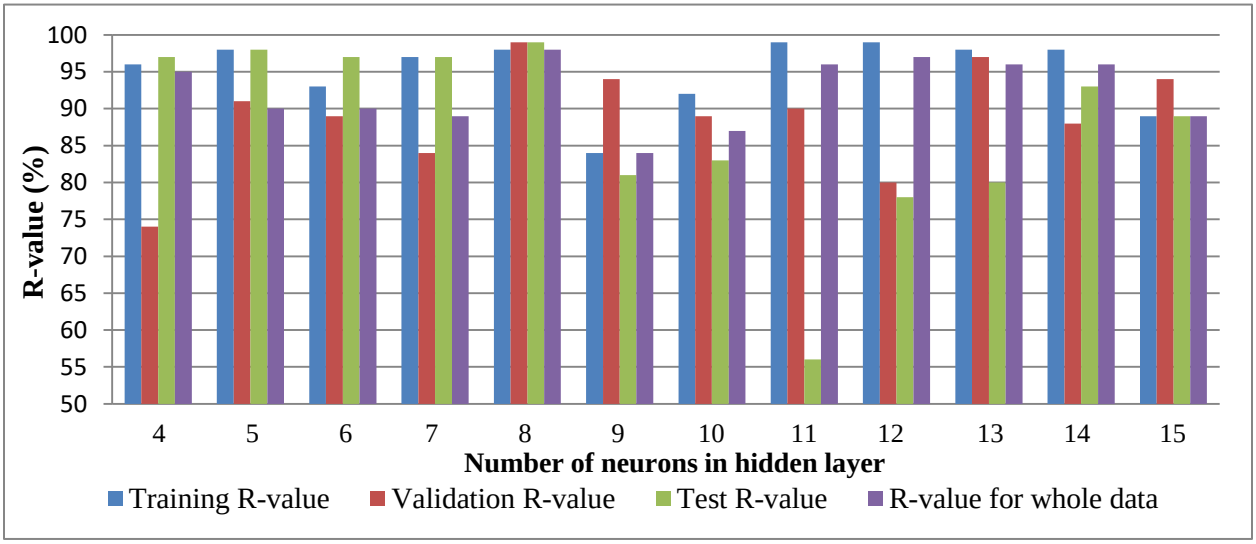

Fig. 2. Regression values for networks with 4–15 neurons in the hidden layer.

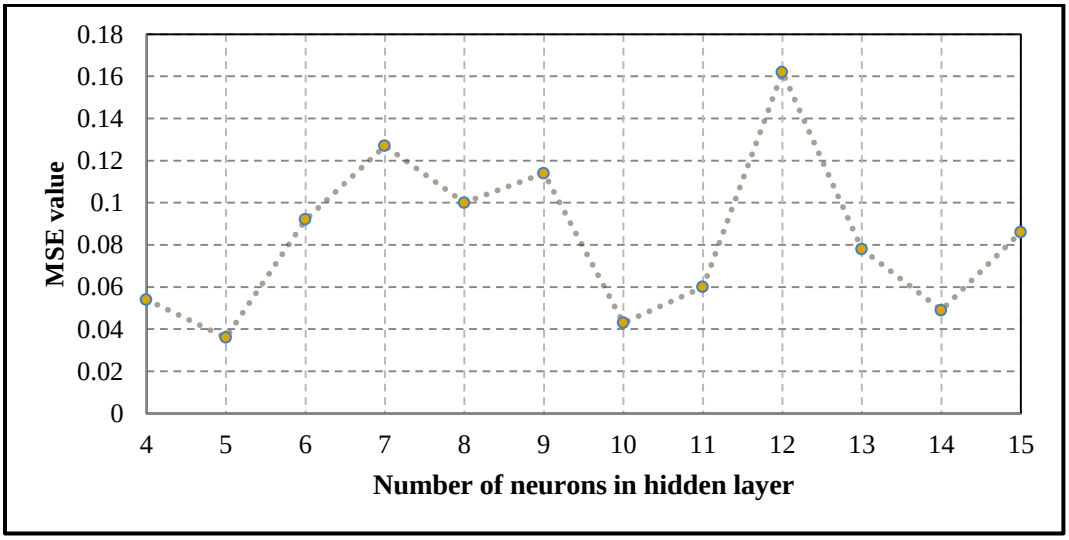

Fig. 3. MSE comparison for networks with 4–15 neurons in the hidden layer.

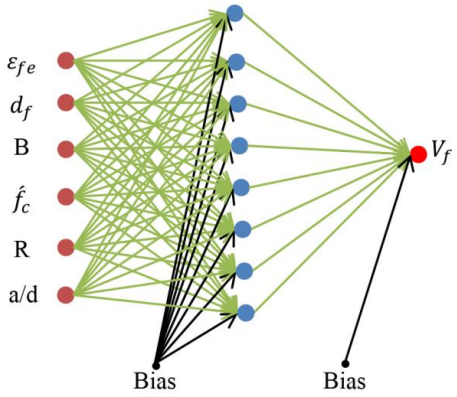

Fig. 4. The architecture of a network with eight neurons in the hidden layer.

The criterion for stopping the training process of the network was Mean Square Error (MSE), which is the average squared difference between outputs and targets. Lower values of MES mean better performance of the network. Regression values (R-values) indicate the relationship between outputs and targets. The maximum value of R-value is 1, and it shows a close relationship between outputs and target values and in contrast, R-value near to 0 means a random relationship. Fig.1, 2 shows the MSE and R-values of networks with different numbers of hidden neurons. The best network is the network which its MSE be lower, and its R-value is higher (network whit eight hidden neurons).

Figs. 4-6 indicate the performance of ANN-8 network. Fig. 5 shows the MSE of the network started at a large value and decreasing to a small value. The plot shows three lines because as mentioned above, the 92 specimens were divided into three groups randomly. Training on the training vectors continues as long as training reduces the error of the network on the validation vectors. When the network memorizes the training set, training is stopped. Fig. 7 indicates the regression values of three sets of data and also the regression of whole data altogether. As it's clear, the regression values show a close relationship between outputs and targets, and it means the network has trained well.

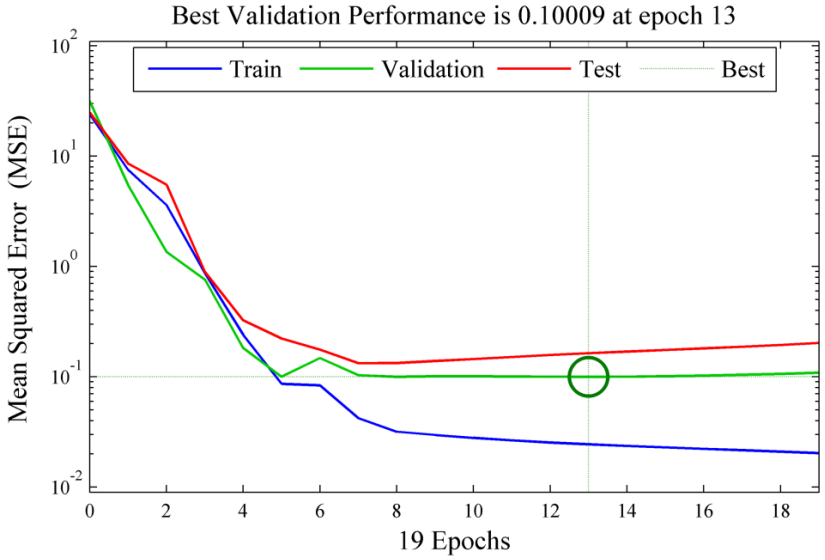

Fig. 5. Mean squared error of ANN-8 network.

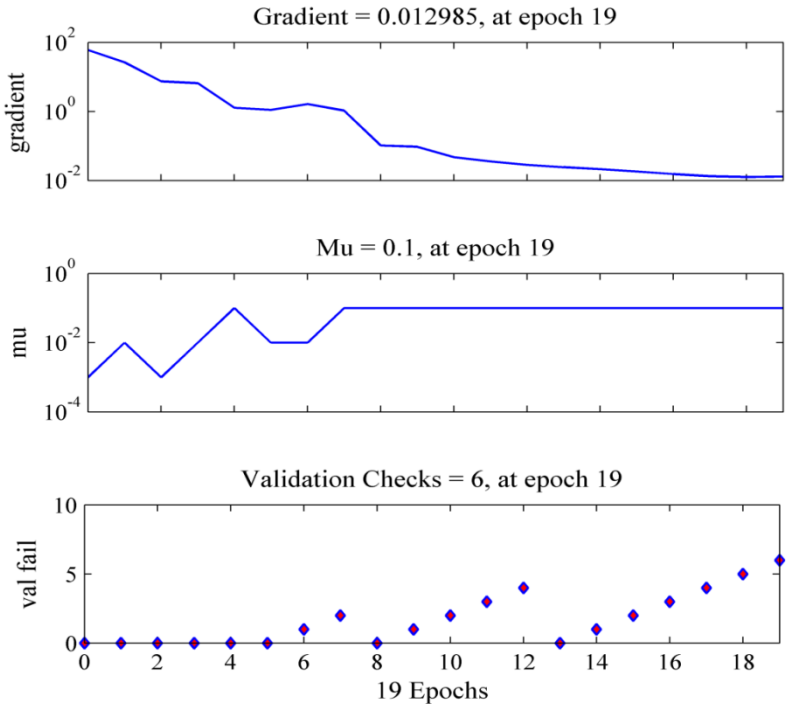

Fig. 6. Training state of ANN-8 network

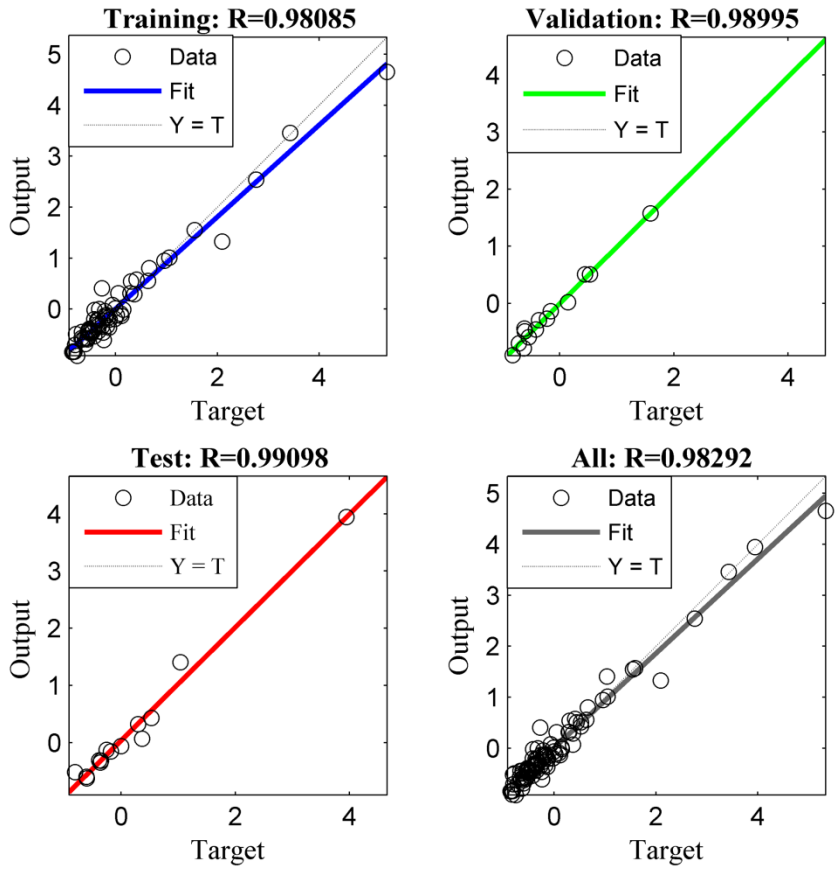

Fig. 7. Regression values for training, validation, and test data.

5. Comparison of ANN Results with Existing Empirical Models

The four common equations for prediction of FRP shear contribution in strengthened RC beams are ACI 440 [14], *fib* bulletin 14 [15], CIDAR [16], and JSCE [17] guidelines. The simulated shear contribution of FRP in strengthened RC beams from the neural network is compared with the prediction of the three existing models, and the result is mapped in fig. 8-12. If there is a perfect agreement between experimental results and the calculated results from the models and network, all point will settle along the 45° line. The error distribution of models and simulated results against experimental results are summarized in Table 7. According to Figs. 8-12 and Table 7, it can be observed that the results of the network have a good agreement with experimental results in comparison with the results of existing models. The mean average error between experimental and prediction results for ANN model, ACI 440, *fib* 14, CIDAR and JSCE equations are equal to 12.9%, 52.9%, 52.6%, 42.9%, and 47.7% respectively. These values indicate that the average error in ANN result is so less than other models. In addition to the mean of errors between experimental results and the predicted results, the Root of Mean Squared Error (RMSE) has calculated for ANN outputs and the results of four other models. ANN model has the minimum RMSE rather than another existing model (Table 8) .Although the average of errors and RMSE can be good for comparison the errors of models, this parameter doesn't indicate the distribution of errors between calculated and experimental values. So for comparison, the distribution of errors, variance of errors around their average has calculated for each equation and also for the ANN model. This parameter for ANN model, ACI 440, *fib* 14, CIDAR and JSCE is equal to 13.3%, 27.1%, 48.6%, 24.3%, 24.1% and 20.1% respectively. These values show that the distribution of errors around the mean error for the ANN model is more uniform than other equations (Table 8).

Table 7. Distribution of errors for different existing models and ANN model.

Range of error (%)	Number of data in the range for models					Percentage to whole data for models (%)				
	ANN model	[14]	[15]	[16]	[17]	ANN model	[14]	[15]	[16]	[17]
±10	49	11	14	5	5	53.3	12.0	15.2	5.4	5.4
±20	76	14	27	6	17	82.6	15.2	29.3	6.5	18.5
±30	83	20	40	15	24	90.2	21.7	43.5	16.3	26.1
±40	85	27	49	17	33	92.4	29.3	53.3	18.5	35.9
±50	89	40	53	22	50	96.7	43.5	57.6	23.9	54.3
±60	92	52	59	29	61	100	56.5	64.1	31.5	66.3
±70	92	72	69	41	79	100	78.3	75.0	44.6	85.9
±80	92	79	77	68	84	100	85.9	83.7	73.9	91.3
±90	92	87	79	89	89	100	94.6	85.9	96.7	96.7
±100	92	89	81	92	90	100	96.7	88.0	100	97.8
±120	92	92	83	92	91	100	100	90.2	100	98.9
±140	92	92	85	92	91	100	100	92.4	100	98.9
±160	92	92	87	92	91	100	100	94.6	100	98.9
±180	92	92	90	92	92	100	100	97.8	100	100
±200	92	92	92	92	92	100	100	100	100	100

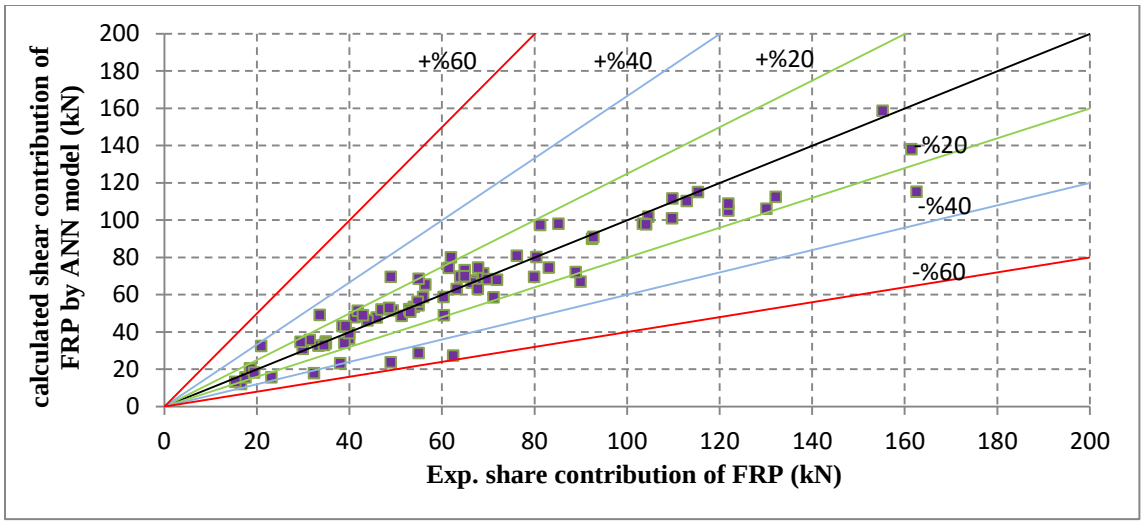

Fig. 8. Comparison between ANN results and experimental values.

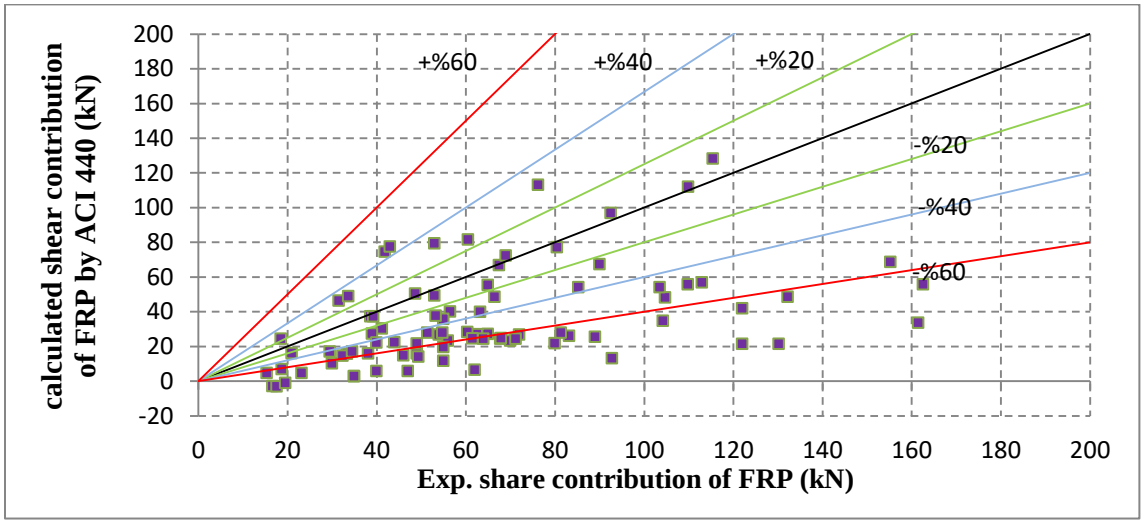

Fig. 9. Comparison between ACI 440 results and experimental values.

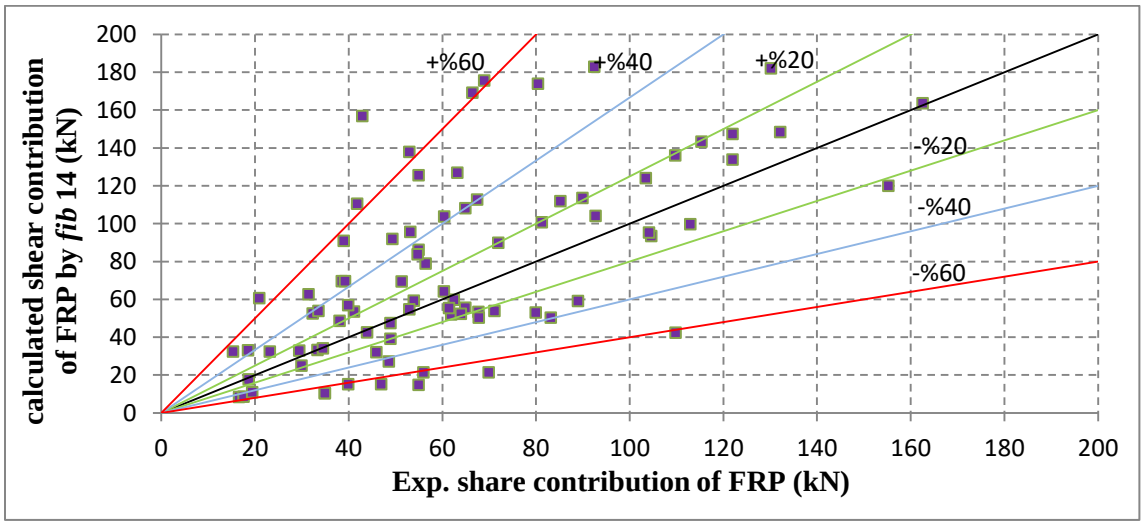

Fig. 10. Comparison between *fib* 14 results and experimental values.

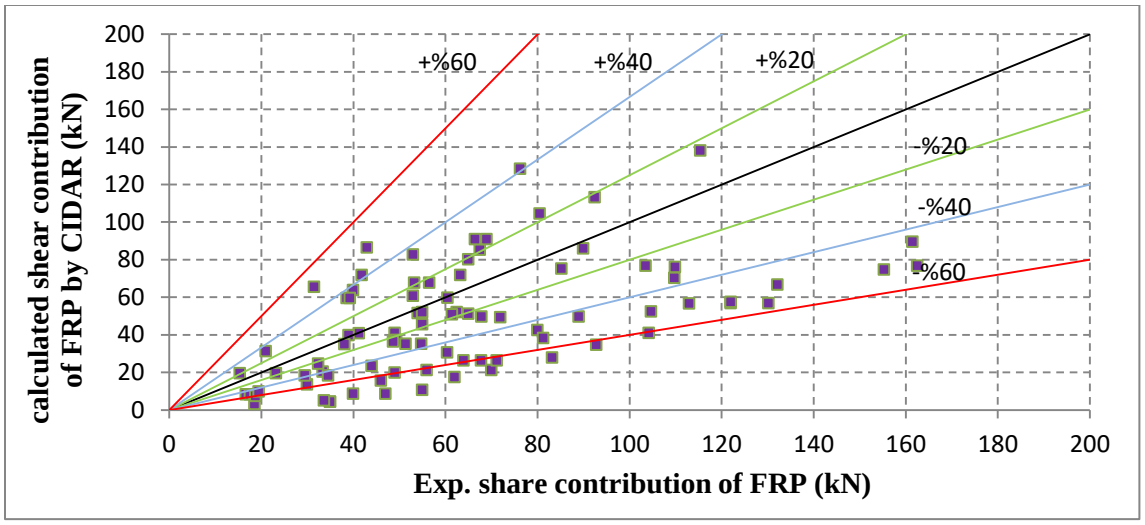

Fig. 11. Comparison between CIDAR results and experimental values.

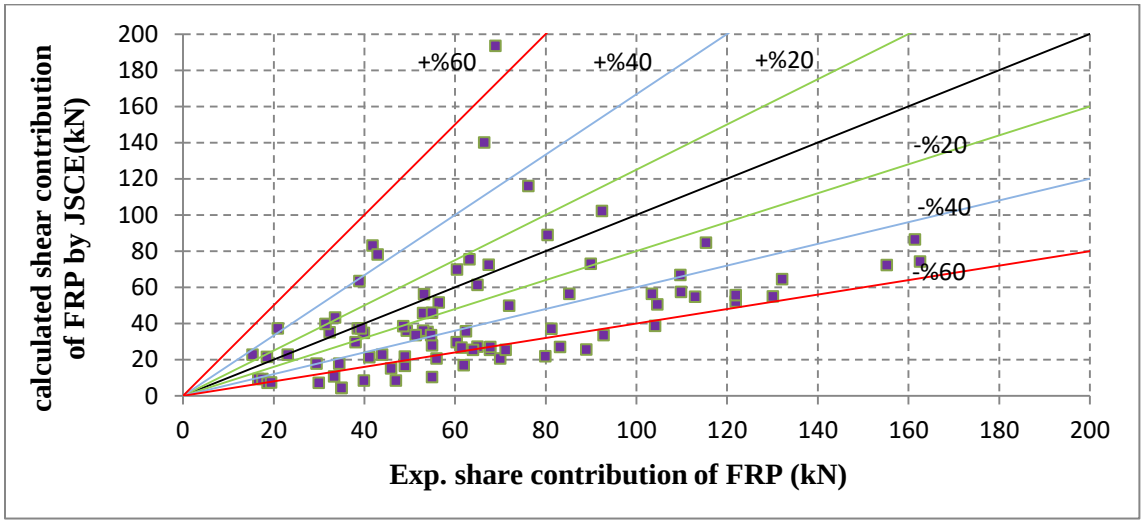

Fig. 12. Comparison between JSCE results and experimental values

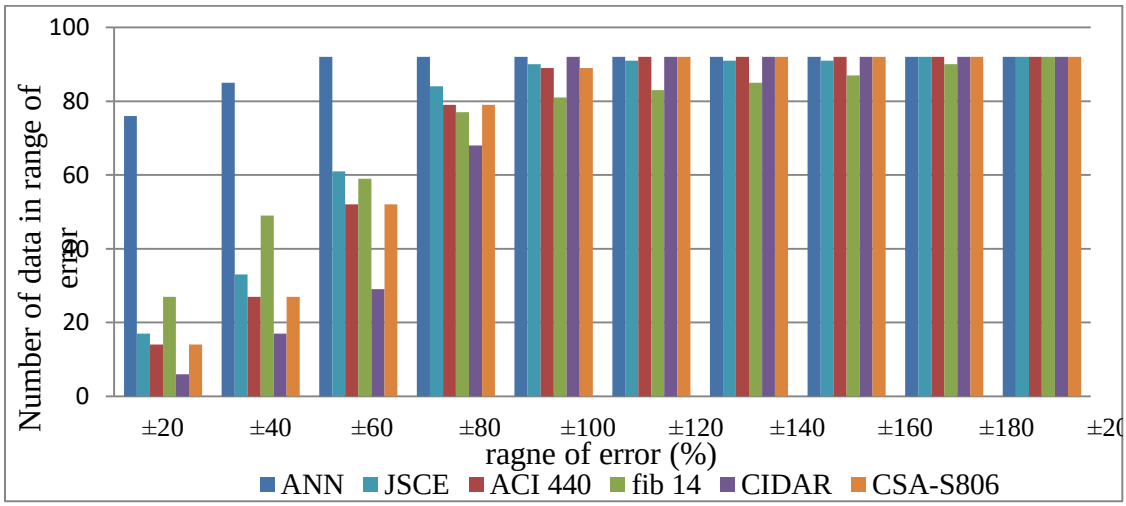

Fig. 13. Comparison between ANN results and other equations predictions.

Table 8. Comparison of average error, RMSE, and variance values between the ANN model and existing model.

Models	Avg. error (%)	RMSE	VAR. (%)
ANN model	12.89	0.19	13.29
ACI 440	52.52	0.59	27.11
fib 14	52.60	0.72	48.62
CIDAR	42.49	0.49	24.1
JSCE	47.72	0.55	20.1

Considering to Table 7 can be determined that more than half of data have an error less than ±10% while the percentage of data which have this amount of error are about 12%, 15% and 5% for ACI 440, *fib* 14 and CIDAR respectively. For controlling the generalization of network performance, the FRP shear contribution of four remained specimens is calculated by existing models and simulated with the network. The results indicated that the proposed network has a good generalization and can perform for other data well. For controlling data, ANN, ACI 440, *fib* 14, and CIDAR code has an average error equal to 17%, 101%, 46%, and 59% respectively. This simulation indicates the generalization of the modeled network and shows that this network can predict the shear contribution of other specimens which it has not trained by them.

6. Sensitivity Analysis

For finding the effect of parameters that have used as input vectors of the network, sensitiveness analyze has done by Garson method and the results according to Eq. (3). In this equation N is the number of input parameters, L is the number of hidden neurons, w_{rj} is the weight which connects input vectors to hidden neurons, and the amount of equation (Q_{ik}) is the importance percentage of each input parameter. This method is based on weights which perform on input parameters and make a relation between them according to target, and the sensitiveness value of each input parameters shows the relative importance of it against other inputs. The results indicate that shear span (a) to the effective depth of beam (d) ratio has the maximum percentage of importance (22.6%) and this parameter plays the main roll in FRP performance, which changing in its value can have a significant effect on shear contribution of FRP. But existing models and equations don't consider this important parameter. Also, width and spacing factor (B) has the minimum effect on shear contribution of FRP between parameters. The results of sensitiveness analyze are summarized in Table 9.

$$Q_{ik} = \frac{\sum_{j=1}^{l}\left(\frac{\left|w_{ij}\right|}{\sum_{r=1}^{N}\left|w_{rj}\right|}v_{jk}\right)}{\sum_{r=1}^{N}\left(\sum_{j=1}^{l}\left(\frac{\left|w_{ij}\right|}{\sum_{r=1}^{N}\left|w_{rj}\right|}v_{jk}\right)\right)} \quad (3)$$

Table 9. The importance of each parameter in sensitiveness analyze.

Parameters	Relative importance
The ultimate strain of FRP (ε_{fu})	(%) 17.3
Effective depth of FRP (d_f)	(%) 16.8
Width and spacing factor B	(%) 9.9
Concrete compressive strength (f'_c)	(%) 12.7
FRP rigidity factor R	(%) 20.7
Shear apan to effective depth (a/d)	(%) 22.6
All	(%) 100.0

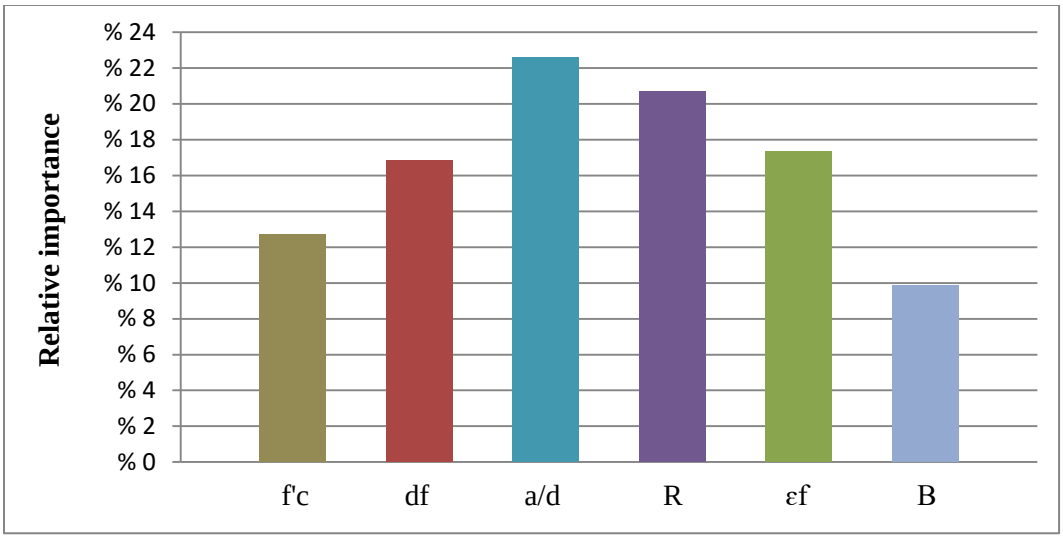

Fig. 14. The relative importance of input parameters on outputs.

7. Conclusion

In this paper, an Artificial Neural Network was presented for estimating the shear contribution of FRP in RC beam strengthened with externally bonded FRP. A set of 92 RC beams were selected as training, validation, and test and four data were used for controlling the generalization the network. One of input parameter was the shear span to the effective depth of beam (a/d) ratio which none of existing models and equations consider to this parameter. The result of comparison ANN model and other models based on experimental is summarized here:

- The average of errors for ANN model, ACI 440, *fib* 14, and CIDAR guidelines is 12.9%, 52.9%, 52.6%, and 61.1% respectively. These values show that the ANN model provides a more accurate result than other models.
- The variance of errors around means error for the ANN model is about 13.3%, which is significantly less than other models. Comparison between the variance of errors indicates that the errors distributed around mean errors of ANN model uniformly.
- More than 50% of whole data have less than 10% error in the ANN model. While the percentage of data with errors equal or less than this amount for ACI 440, *fib* 14 and CIDAR is 12%,15%, and 5% respectively.
- A sensitiveness analyze has performed for finding out the importance of each input parameter on network output by Garson method. The results indicated that the shear span to the effective depth of beam (a/d) has the maximum effect on the contribution of FRP while the width and spacing parameters (B) has the minimum effect.

Notation

A_{FRP} = area of FRP shear reinforcement;

b_w = minimum width of RC beam;

D_{FRP} = stress distribution factor in FRP;

d = effective depth of the cross section;

d_{FRP} = effective depth of the FRP shear reinforcement_usually equal to d for

rectangular sections and (d-thickness) of the slab for T sections;

$d_{FRP,t}$ = distance from the compression face to the top edge of the FRP;

E_{FRP} = Young's modulus of the FRP;

f_c = compressive strength of concrete;

f_{FRP} = tensile strength of FRP;

h = height of the beam;

$d_{FRP,e}$ = effective height of FRP;

L_e = effective bond length;

S_{FRP} = center to center spacing of FRP strips measured along longitudinal axis;

t_{FRP} = thickness of FRP shear reinforcement;

w_{FRP} = width of FRP;

α = fiber angle direction with respect to the longitudinal axis of the beam;

β_L = bond length coefficient;

β_w = strip width coefficient;

$\mathbf{g}_b$ = partial safety factor for bond strength, equals 1.25;

$\boldsymbol{\varepsilon}_{FRP,e}$ = effective FRP strain in principal fiber direction;

$\boldsymbol{\varepsilon}_{FRP,u}$ = ultimate tensile strain in FRP;

θ = crack angle direction with respect to the longitudinal axis of the beam;

$\mathbf{r}_{FRP}$ = FRP shear reinforcement ratio;

$\boldsymbol{\varepsilon}_{FRP,max}$ = maximum stress in FRP;

REFERENCES

[1] Täljsten, B., Strengthening concrete beams for shear with CFRP sheets, Construction and Building Materials, 2003, 17, 15–26.

[2] Triantafillou, T. C., COMPOSITES: A NEW POSSIBILITY FOR THE SHEAR STRENGTHENING OF CONCRETE, MASONRY AND WOOD, Composites Science and Technology 1998, 58, 1285-1295.

[3] Li, A., Diagana, C., Delmas. Y., CRFP contribution to shear capacity of strengthened RC beams, Engineering Structures 2001, 23, 1212–1220.

[4] Chen, J. F., Teng, J. G., Shear Capacity of Fiber-Reinforced Polymer-Strengthened Reinforced Concrete Beams: Fiber Reinforced Polymer Rupture, ASCE Structural Engineering. 2003, 129, 615-625.

[5] Berset, J. D., Strengthening of Reinforced Concrete Beams for Shear Using FRP Composites, M.Sc. thesis, Massachusetts Institute of Technology, Jan. 1992.

[6] Uji, K., Improving shear capacity of existing reinforced concrete members by applying carbon fiber sheets. Trans. Japan Concrete Institute, 1992, 14, 253-266.

[7] Vielhaber, J. and Limberger, E., Upgrading of Concrete Beams with a Local Lack of Shear Reinforcement, Federal Institute for Materials Research and Testing (BAM), Unpublished Report, Berlin, Germany, 1995.

[8] Chajes, M. J., Januska, T. F., Mertz, D. R., Thomson, T. A. and Finch, W. W., Shear strengthening of reinforced concrete beams using externally applied composite fabrics. ACI Structural Journal, 1995, 92, 295-303.

[9] Sato, Y., Ueda, T., Kakuta, Y. and Tanaka, T., Shear reinforcing effect of carbon fiber sheet attached to side of reinforced concrete beams. In Advanced Composite Materials in Bridges and Structures, ed. M. M. El-Badry, 1996, 621-627.

[10] Gamino, A. L., Sousa, J. L. A. O., Manzoli, O. L., Bittencourt, T. N., Estruturas de Concreto Reforçadas com PRFC, Part II: Análise dos Modelos de Cisalhamento, Ibracon Structures and Materials Journal, 2010, 3, 24-49.

[11] Teng, J. G., Chen, G. M., Chen, J. F., Rosenboom, O. A., Lam, L., Behavior of RC Beams Shear Strengthened with Bonded or Unbonded FRP Wraps, Compos. Constr., 2009, 13, 394-404.

[12] Bousselham, A., Chaallal, O., Effect of transverse steel and shear span on the

performance of RC beams strengthened in shear with CFRP, Composites: Part B 2006, 37, 37–46.

[13] Naderpour, H., Kheyroddin, A., Ghodrati Amiri, G., Prediction of FRP-confined compressive strength of concrete using artificial neural networks, Composite Structures, 2010, 92 (12), 2817-2829.

[14] ACI Committee 440 Report, Guide for the design and strengthening of externally bonded FRP systems for strengthening concrete structures. American Concrete Institute Committee; October 2001.

[15] Fib. Bulletin 14, externally bonded FRP reinforcement for RC structures. Technical report. Task Group 9.3 FRP (fibre reinforced polymer) reinforcement for concrete structures; 2001.

[16] CIDAR, Design guideline for RC structures retrofitted with FRP and metal plates: beams and slabs. Draft 3 – submitted to Standards Australia, The University of Adelaide; 2006.

[17] JSCE, RECOMMENDATIONS FOR UPGRADING OF CONCRETE STRUCTURES WITH USE OF CONTINUOUS FIBER SHEETS, Japan strengthening with FRP guideline.

[18] Triantafillou, TC., Shear strengthening of reinforced concrete beams using

[19] Epoxy-bonded FRP composites, ACI Struct. J 1998, 95, 107–15.

[20] Chaallal, O., Nollet, M.-J., and Perraton, D. 1998. “Strengthening of reinforced concrete beams with externally bonded fibre-reinforcedplastic plates: Design guidelines for shear and flexure.” Can. J. Civ. Eng., 25, 692–708.

[21] Christopher, K. Y., Leung, M., Mandy, Y. M., Herman, C. Y., Empirical Approach for Determining Ultimate FRP Strain in FRP-Strengthened Concrete Beams, composites for construction, 2006, 10, 125-138.